



OPEN

Localized shear deformation and softening of bulk metallic glass: stress or temperature driven?

SUBJECT AREAS:

GLASSES

MECHANICAL PROPERTIES

Received

23 July 2013

Accepted

6 September 2013

Published

8 October 2013

Correspondence and requests for materials should be addressed to K.S.V. (ketov.sergey@wpi-aimr.tohoku.ac.jp)

Ketov S. V. & Louzguine-Luzgin D. V.

WPI Advanced Institute for Materials Research, Tohoku University, Japan 2-1-1, Katahira, Aoba-ku, Sendai, Miyagi, 980-8577, Japan.

Metallic glasses due to their unique combination of physical and chemical properties have a great potential in various applications: materials for construction, medical, MEMs devices and so on. The deformation mechanism in metallic glasses is very much different from that in conventional crystalline materials and not yet fully understood. Here we are trying to find out what drives shear deformation in metallic glasses. The compression experiments of the bulk metallic glassy (BMG) samples coated with tin, Rose metal and indium were performed. There were no melting sites of the coating observed near individual shear bands. Melting occurred only near fracture surface, near microcracks and in the places of shear band concentrations. The results indicate that shear banding is rather a stress driven process while the temperature rise that was observed takes place due to friction forces in the viscous supercooled liquid thin layer in the shear bands.

Metallic glasses due to their good mechanical properties are promising structural materials. High yield stress, good wear and corrosion resistance, good soft magnetic properties, etc. make them useful in various applications¹⁻³. In general, the deformation mechanism in metallic glasses at room temperature is very different from conventional crystalline materials and had not been fully understood yet. With the difference in size and temperature of the sample, bulk metallic glasses (BMG) could undergo either homogeneous or inhomogeneous plastic deformation^{4,5}. There are several theories which explain inhomogeneous plastic deformation of BMGs from different points of view. One of them involves existence of shear transformation zones (STZ) or their creation upon the beginning of deformation^{6,7}. With the increase in stress STZs create a localized distortion of the surrounding material, which triggers the formation of very thin and planar bands of STZs known as “shear bands”. Dynamics of the formation and propagation of these shear bands upon the deformation is now the subject of wide dispute⁶⁻⁹. Either they are driven by internal structure changes due to work softening under stress or there is a temperature rise in them above the glass-transition temperature of the BMG sample before plastic deformation which in turn allows shear bands propagation. One should note that thicker shear bands were observed on severe plastic deformation of crystalline alloys as well, but this is not a common deformation mechanism in such materials.

In several works it was shown¹⁰⁻¹² that there is a rise of temperature in the shear bands of BMGs. In the work¹⁰ using four-point bending of the Zr-based BMG coated by sputtered tin nanoparticles J. Levandovski and A. Greer showed that creation and propagation of shear bands cause the local temperature rising in the BMG sample along them and the appropriate calculations of the temperature rise were provided. These calculations gave very high values of temperature in the center of a shear band up to 3,100–8,300 K depending on the duration of shear. However, as one can see from the images Sn coating melting was mostly observed in the places of shear band concentrations and near cracks. In the present research we tried to improve this technique by using alloys and elements with lower melting temperature for coating a BMG sample which demonstrates a rather high plasticity at room temperature.

Results

Sputtering of different substances on both ribbons and bulk samples lead to the formation of nanoparticle coating. The average size of the particles in case of each substance was 20–100 nm. Ribbon samples were bended until plastic deformation occurred. For bending test inner (compression) side of the ribbon was coated. From SEM images one can see that neither pure elements nor Rose metal coatings clearly melted near the shear bands (fig. 1).

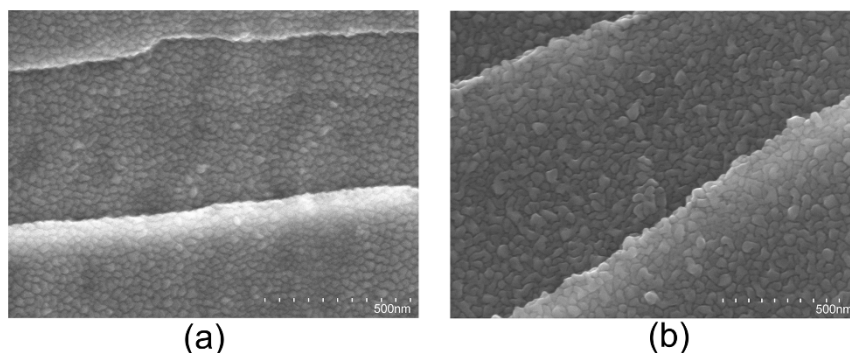


Figure 1 | Shear bands exits on the ribbon surface coated by indium (a), Rose metal (b).

On the SEM image fig. 2 we can see that after compression tests of the bulk samples there are also no clear melting sites near a single shear band exits. There are several sites in which we could see shear band crossing Rose metal particle (Fig. 2b). The final shape of the particle implies that it was melted but the evidence is not solid.

After that the compression tests on the bulk samples were done until their catastrophic failure. In some places near the fracture surface one could notice clear signs of melting of Rose metal and indium (fig. 3), but not along the whole surface. Some parts were looked intact.

Tin coating did not melt almost all over the boundary of the fracture surface and even near the big cracks the coating was intact (fig. 4a, b). There are only few places where tin coating melting could be found. All of them mostly were the concentration places of several shear bands and cracks (fig. 4c, d).

Discussion

The results of our experiments are in agreement with the calculations done by Miracle et. al.¹³. They have shown that the shear offset (δ) is proportional to the size of the sample (D) and heat content of the shear band is proportional to the shear stress and shear offset. As one

can see (Fig. 1) the shear offsets in ribbon samples are very small (less than $1 \mu\text{m}$) and heat content of these shear bands is not enough to melt even Rose metal particles with the lowest melting temperature. However, the same situation was also observed in the bulk samples after the compression test. With the increase in the sample size and shear offset we could not see clear melting of coating near a single shear band. Even near the fracture surface clear melting sites are rare (this effect is likely connected with crack propagation speed variation upon fracture¹⁴) and could be seen only near cracks and shear bands concentrations where local heat release is high enough to cause the coating melting.

If we apply equations from Ref. 11 to our BMG alloy (Table 1), the maximum half-thickness of the zone with reference temperature (here it is the melting point of tin $T_L = 505 \text{ K}$) would be:

$$x_{\text{max}} = \beta Z \delta, \quad (1)$$

where β is a constant of maximum value 0.5^{11} , δ is the shear offset and parameter Z depends only from the material and equals to:

$$Z = \frac{1}{\sqrt{2\pi e}} \left(\frac{\sigma_y}{T_L \rho C} \right) \quad (2)$$

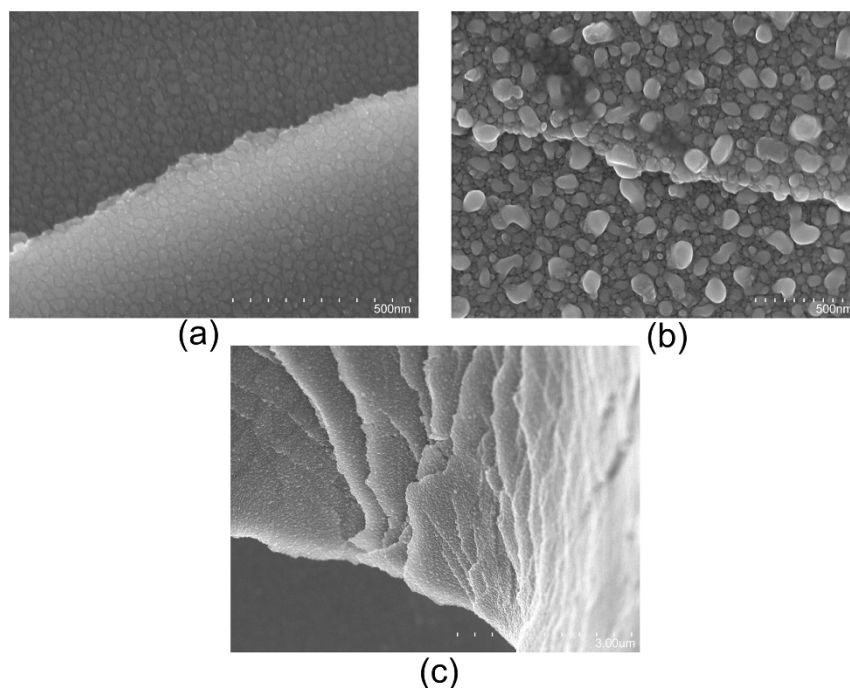


Figure 2 | SEM images of the shear band exits on the bulk sample surface coated by indium (a), Rose metal (b) and tin (c) after the compression test.

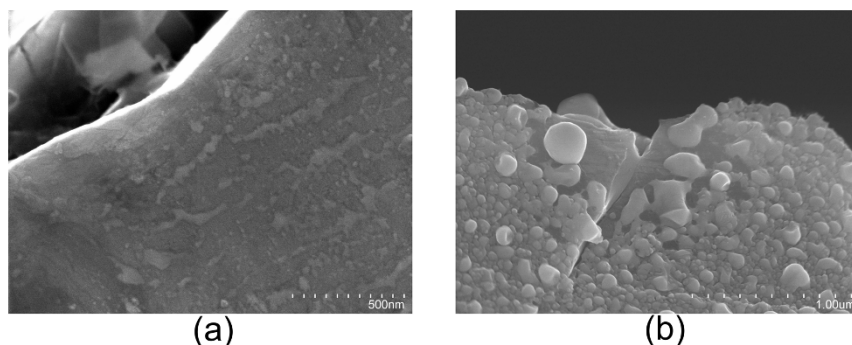


Figure 3 | SEM images the areas near the fracture surface of the bulk sample coated by indium (a), Rose metal (b) after the compression test.

For shear bands with the shear offset $\delta = 1 \mu\text{m}$ and $\beta = 0.3$ maximum half-thickness of the melted zone should be 80 nm. But shear offset $\delta = 1 \mu\text{m}$ is very small and there are shear bands with offsets more than $10 \mu\text{m}$ for which half-thickness of the melted zone would be $x_{\text{max}} \sim 10^2 \text{ nm}$. In the work¹³ the equations were derived in assumption that heating is instantaneous and shear band operation time (τ) was not accounted for, while it is clear that parameter β in these equations should depend on τ .

The operation time of the shear bands is still a question to debate. Several works were performed to determine the actual shear band propagation speed^{16–19}. Using highly sensitive strain gages and high speed data acquisition machines they found out that the shear band speed is about 10^{-4} – 10^{-3} m/s (or for shear step $1 \mu\text{m}$, $\tau \sim 10^{-2} \text{ sec}$) which is way below the estimated value for the temperature rise needed. However, this speed was estimated for the shear band that allows sliding of one part of the specimen over another. If we assume that shear displacement occurs as a localized front that propagates across the specimen, than shear band speed would be 10^1 m/s which is enough to rise the local temperature to the values above the T_g . At the same time, the experiment with filming the propagation of the shear band with high speed camera¹⁸ showed that in such

conditions the whole shear event took place simultaneously over the entire shear plane.

There is another approach to the shear band operation. In the work²⁰ Guan et al. suggested that there is a coupling between temperature and shear stress. This means that softening of the glassy phase leading to deformation of the sample could be explained either by temperature rising or by applying stress. Also in the work¹⁷ Song and Nieh tried to explain shear band deformation by free volume model. They reported that the viscosity value at the measured shear band speed in the BMGs deformed with strain rates of 10^{-5} s^{-1} is about 10^4 – $10^5 \text{ Pa}\cdot\text{s}$. These values are common for the supercooled region temperature of BMG. Applying the free volume model for the shear band viscosity measured at room temperature Song and Nieh showed that a sharp increase of the excess free volume at yielding is mainly responsible for the low viscosity of a propagating shear band. The viscosity and strain rate data can be well described by the self-consistent VFT equation based on a free volume model. The strain rate in the shear band during its operation (10^3 – 10^4 s^{-1}) obtained in¹⁶ also correlates well with the results of the work²¹. It was shown that with the increase of the overall macroscopic compression strain rate, plasticity of the BMG sample lowered and at the point when the

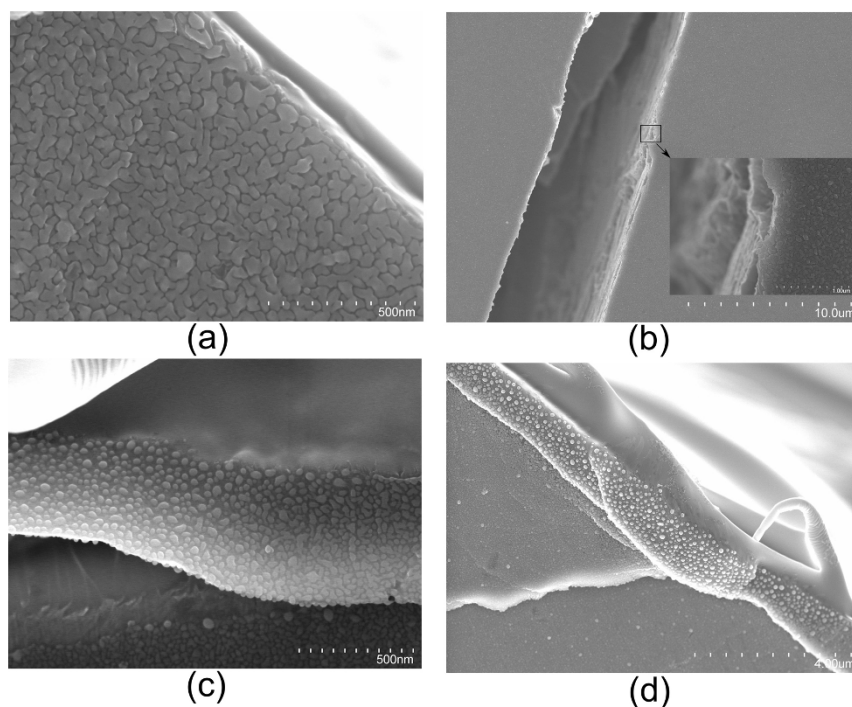


Figure 4 | SEM images the areas near the fracture surface of the bulk sample coated by tin after the compression test.



Table 1 | Alloy properties

Specific heat capacity C_p (J/kg K)	Density, ρ (kg/m ³)	Yield stress, σ_y (MPa)	Glass transition temperature T_g (K)	Liquidus temperature T_{liq} (K)
390	6847	1475	650 ¹⁵	1173 ¹⁵

macroscopic compression strain rate has reached the values of the strain rate in the shear band (10^3 s^{-1}) in dynamic loading experiment macroscopic plasticity dropped to zero due to the lack of time for stress relaxation. Thus, at low strain rates during deformation BMG sample has enough time to nucleate new shear bands and one could see a lot of shear bands offsets on the surface and observe overall high plasticity^{21,22}. With the increase of the strain rate the number of shear bands exiting on the surface is decreasing and most of the deformation is going through a small number of initially nucleated shear bands and we observe decrease of plasticity. Thus, in relatively ductile BMGs at the point when the overall strain rate reaches the value equal to the strain rate in the shear band we observe fracture through the first nucleated shear band.

We suppose that shear softening and localized deformation in shear bands is most likely a stress-driven process. Such an assumption explains the typical serrated flow shown in Fig. 5b. Propagation of a shear band starts at some critical shear stress value, which is highly constant for a specimen of a certain size and a volume fraction of defects (Fig. 5a). This value is quite stable in terms of true stress value until a single dominant shear band is formed²³. Stoppage of the shear band propagation takes place when the stress drops below a certain value when it is not high enough to maintain plastic deformation and a subsequent rise of stress is necessary. The initial rise of

stress at small deformation is likely connected with geometrical imperfectness of the cuboid sample.

But one could ask, what about the temperature rise in the shear bands that was observed by infrared cameras^{12,22}? Even having such low values of the viscosity at calculated shear speed there is a high friction force in the shear band. To estimate the temperature rise due to the friction force in the shear band we made the following assumptions: deformation takes place only in the liquid layer and there is only internal liquid friction. Also, we do not consider friction between liquid and solid glassy phases and suggest that the whole work against friction force transforms into heat. Considering that the shear event takes place simultaneously over the entire shear plane and that heat transfer in the liquid phase is instantaneous due to its very small thickness we can say that heat release (H) (J m^{-2}) is given by:

$$H = \frac{F \cdot \delta}{S}, \quad (3)$$

where F is the friction force in liquid, δ – the shear offset, S – the shear area.

As it is known the friction force in liquid:

$$F = \eta \cdot \frac{v \cdot S}{h}, \quad (4)$$

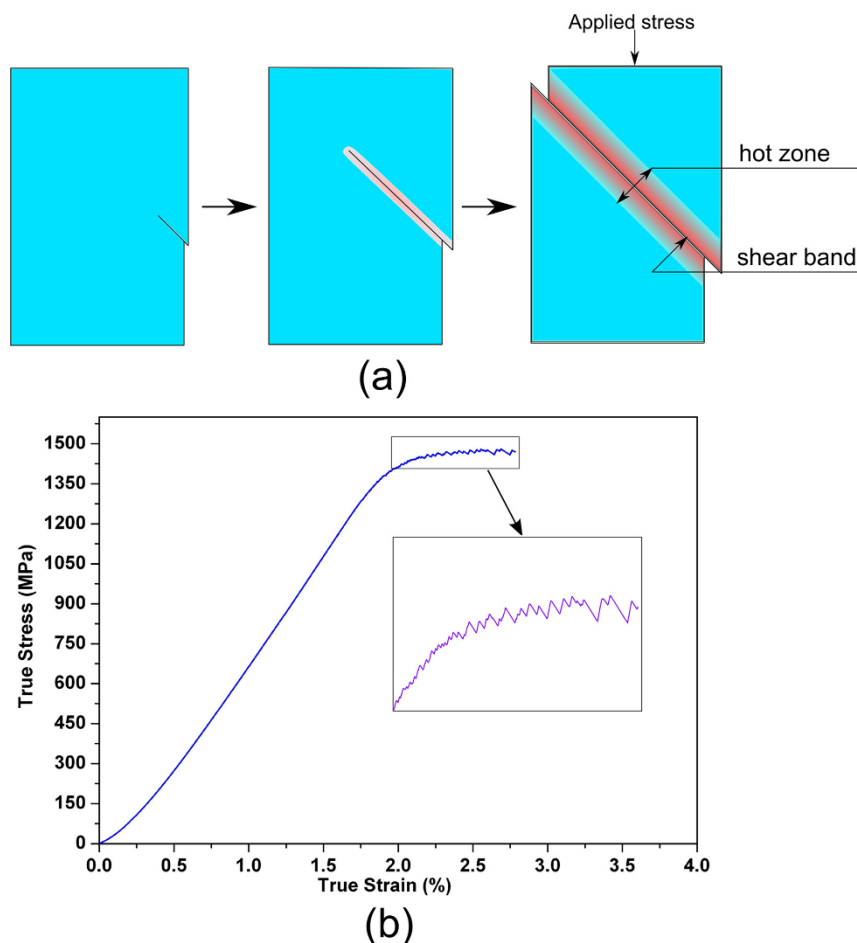


Figure 5 | Schematic view of the deformation process in BMG sample (a), typical true stress-strain curve of the bulk glassy sample obtained at the strain rate of $5 \cdot 10^{-4} \text{ s}^{-1}$ (b).



where η is liquid viscosity, v – shear band velocity, h – liquid zone thickness.

Taking into account equation (4) heat release H will be:

$$H = \frac{\eta \cdot v \cdot \delta}{h} \quad (5)$$

Taking into account thin plate heat source solution for the diffusion equation¹⁰ the evolution of temperature profile after shear would be:

$$\Delta T = \left(\frac{H}{2\rho C_p \sqrt{\pi \alpha}} \right) \frac{1}{\sqrt{t}} \exp\left(-\frac{x^2}{4\alpha t}\right), \quad (6)$$

where ΔT is the temperature rise above ambient at a distance x from the heat source, ρ , C_p and α are, respectively, the density, specific heat capacity, and thermal diffusivity of the metallic glass; and t is the time elapsed since the end of shear. As the time passes the temperature at some distance from a shear band first rises then falls. So the distance x_{\max} of a certain temperature rise ΔT_{ref} at given time would be:

$$x_{\max} = \frac{1}{\sqrt{2\pi e}} \left(\frac{H}{\rho C_p} \right) \frac{1}{\Delta T_{\text{ref}}}, \quad (7)$$

Considering viscosity in the liquid of 10^4 Pa*s, shear band velocity of 10^{-4} m*s⁻¹¹⁸, shear offset of 10^{-6} m, and liquid zone thickness of 10^{-8} m for $\Delta T_c = 505$ K (melting point of tin) the distance x_{\max} would be about 10 nm which is not enough to melt the tin coating grain of about 50 nm in size. The same considerations could be applied for the Rose alloy and In coatings.

Local heating in shear bands is usually observed by infrared cameras¹² but their spatial and time resolutions are not high enough to catch a single shear band propagation. Considering that space and time resolution are $x = 15$ μm , $t = 2.5$ ms, respectively, and thermal diffusivity coefficient of the metallic glass estimation $\alpha = 2 \cdot 10^{-6}$ m²s⁻¹²⁴ from equation (6) we can show that the temperature rise that could be detected by an IR camera is several degrees Kelvin as was obtained in several works^{12,25,26}.

In a recent work by Z. Y. Liu et al.²⁷ it was found out that propagation speed of a shear band correlates with the shear offset. This result is consistent with our work and work of Lewandowski and Greer¹⁰ because with rising velocity of shear band friction forces are rising too, and at some point of a large shear offset or near shear band concentration places, the temperature can achieve the melting point of Sn, In or Rose alloy. The results of the work²⁷ are also in good correlation with the work²⁶. The authors found that the temperature rise in a shear band increases with increasing strain rates, demonstrating their strain-rate dependence. As we mentioned above with increase in an overall macroscopic compression strain rate the number of shear bands lowers and their surface offset values increase. Thus, with increasing of the offset values, the velocity of shear bands is also increasing²⁵ as well as the temperature in the shear band²⁸. When the temperature rises by friction force energy release, the thickness of the low viscosity region increases and at some critical point the sample breaks down. This process is clearly stochastic and can depend on the internal structure of individual sample²³. Stochastic formation of a dominant shear band with large critical offset is leading to an overcritical rise in temperature which in turn becomes the cause of early sample's break down. That's why samples of the same chemical origin demonstrate significantly different plasticity in various experiments.

In conclusion, the bend and compression experiments of the ribbon and BMG samples coated with different materials were performed. There was no coating melting observed near individual shear bands. Melting occurred only in some places near the fracture surface, near microcracks and near the places of shear band concentrations where total heat release was large enough to initiate melting. It is suggested that in fact shear localization and banding is a stress driven process and the temperature rise that was observed in the

shear bands is due to the friction forces in the thin liquid layer within the shear bands. Numerical calculations support this conclusion.

Methods

Compression test experiments were done on the Zr_{62.5}Cu_{22.5}Al₁₀Fe₃ BMG coated by tin element having liquidus temperature (T_L) of 505 K, indium ($T_L = 430$ K) and Rose alloy (Bi₅₀Pb₂₆Sn₂₄ at.%, $T_L = 372$ K). Initial BMG alloy was prepared by arc melting of the high purity elements (99.9 mass.% purity) under an argon atmosphere. From the ingot, 45 mm long rectangular parallelepipeds of 2×3 mm in cross section were casted into Cu-mould. Also ribbon samples of about 20 μm in thickness were prepared by low pressure Ar casting on a rolling copper wheel. Coating has been done by a magnetron sputtering technique with initial pressure inside the chamber of 10^{-4} Pa from high purity elements (99.99 mass.% purity) and commercial Rose alloy. The structure and phase composition of the samples were examined by scanning electron microscopy (SEM Hitachi S-4800), x-ray diffraction (XRD) with Cu K α radiation (Bruker D8 Advance). Mechanical tests were carried out using an Instron-type (Shimadzu AG-50 kN-Xplus) testing machine. Phase transformations were studied and specific heat capacity measurements were done by differential scanning calorimetry machines Seiko Instr. Inc. DSC 6300 Exstar and Perkin Elmer DSC 8500, respectively. Sample density was measured by the Archimedeian method.

- Louzguine-Luzgin, D. V. & Inoue, A. Bulk Metallic Glasses. Formation, Structure, Properties, and Applications. *Handbook of Magnetic Materials* **21**, 131 (2013).
- Suryanarayana, C. & Inoue, A. Iron-based bulk metallic glasses. *International Mat. Rev.* **58**(3), 131 (2013).
- Wang, J. Q., Liu, Y. H., Chen, M. W., Louzguine-Luzgin, D. V., Inoue, A. & Perepezko, J. H. Excellent capability in degrading azo dyes by MgZn-based metallic glass powders. *Sci Rep.* **2**, 418 (2012).
- Ketov, S. V., Chen, N., Caron, A., Inoue, A. & Louzguine-Luzgin, D. V. Structural features and high quasi-static strain rate sensitivity of Au₄₉Cu_{26.9}Ag_{5.5}Pd_{2.3}Si_{16.3} bulk metallic glass. *Appl. Phys. Lett.* **101**, 241905 (2012).
- Song, S. X., Lai, Y. H., Huang, J. C. & Nieh, T. G. Homogeneous deformation of Au-based metallic glass micropillars in compression at elevated temperatures. *Appl. Phys. Lett.* **94**, 061911 (2009).
- Schuh, C., Hufnagel, T. & Ramamurty, U. Mechanical behavior of amorphous alloys. *Acta Mater.* **55**(12), 4067 (2007).
- Trexler, M. M. & Thadhani, N. N. Mechanical properties of bulk metallic glasses. *Prog. Mater. Sci.* **55**, 759–839 (2010).
- Bokeloh, J., Divinski, S. V., Reglitz, G. & Wilde, G. Tracer measurements of atomic diffusion inside shear bands of a bulk metallic glass. *Phys. Rev. Lett.* **107**, 235503 (2011).
- Greer, A. L., Cheng, Y. Q. & Ma, E. Shear bands in metallic glasses. *Mat. Sci. and Eng. R* **74**, 71–132 (2013).
- Lewandowski, J. J. & Greer, A. L. Temperature rise at shear bands in metallic glasses. *Nature mat.* **5**, 15–18 (2006).
- Zhang, Y. et al. Local temperature rises during mechanical testing of metallic glasses. *J. Mater. Res.* **22**(2), 419–427 (2007).
- Wang, G. et al. Thermographic studies of temperature evolutions in bulk metallic glasses: An overview. *Intermetallics* **30**, 1–11 (2012).
- Miracle, D. B., Concustell, A., Zhang, Y., Yavari, A. R. & Greer, A. L. Shear bands in metallic glasses: Size effects on thermal profiles. *Acta Mater.* **59**, 2831–2840 (2011).
- Chen, N., Louzguine-Luzgin, D. V., Xie, G. Q. & Inoue, A. Nanoscale wavy fracture surface of a Pd-based bulk metallic glass. *Appl. Phys. Lett.* **94**, 131906 (2009).
- Louzguine-Luzgin, D. V., Xie, G., Zhang, Q. & Inoue, A. Effect of Fe on the glass-forming ability, structure and devitrification behavior of Zr-Cu-Al bulk glass-forming alloys. *Philosophical Mag.* **90**(14), 1955–1968 (2010).
- Wright, W. J., Samale, M. W., Hufnagel, T. C., LeBlanc, M. M. & Florando, J. N. Studies of shear band velocity using spatially and temporally resolved measurements of strain during quasistatic compression of a bulk metallic glass. *Acta Mater.* **57**, 4639–4648 (2009).
- Song, S. X. & Nieh, T. G. Flow serration and shear-band viscosity during inhomogeneous deformation of a Zr-based bulk metallic glass. *Intermetallics* **17**, 762–767 (2009).
- Song, S. X., Wang, X.-L. & Nieh, T. G. Capturing shear band propagation in a Zr-based metallic glass using a high-speed camera. *Scripta Mater.* **62**, 847–850 (2010).
- Chen, H. M., Huang, J. C., Song, S. X., Nieh, T. G. & Jang, J. S. C. Flow serration and shear-band propagation in bulk metallic glasses. *Appl. Phys. Lett.* **94**, 141914 (2009).
- Guan, P., Chen, M. & Egami, T. Stress-temperature scaling for steady-state flow in metallic glasses. *PRL* **104**, 205701 (2010).
- Ma, W., Kou, H., Li, J., Chang, H. & Zhou, L. Effect of strain rate on compressive behavior of Ti-based bulk metallic glass at room temperature. *J. of Alloys and Compd.* **472**, 214–218 (2009).
- Jiang, W. H. et al. Spatiotemporally inhomogeneous plastic flow of a bulk-metallic glass. *Inter. J. of Plast.* **24**, 1–16 (2008).
- Louzguine-Luzgin, D. V., Packwood, D. M., Xie, G. & Churyumov, A. Yu. On deformation behavior of a Ni-based bulk metallic glass produced by flux treatment. *J. of Alloys and Compd.* **561**, 241–246 (2013).
- Yamasaki, M., Kagao, Sh. & Kawamura, Yo. Thermal diffusivity and conductivity of Zr₅₅Al₁₀Ni₅Cu₃₀ bulk metallic glass. *Scripta Mater.* **53**, 63–67 (2005).



25. Yang, B. *et al.* In-situ thermographic observation of mechanical damage in bulk-metallic glasses during fatigue and tensile experiments. *Intermetallics* **12**, 1265–74 (2004).
26. Jiang, W. H., Liao, H. H., Liu, F. X., Choo, H. & Liaw, P. K. Rate-dependent temperature increases in shear bands of a bulk-metallic glass. *Metallurgical and Mater. Trans. A* **39A**, 1822–30 (2008).
27. Liu, Z. Y., Yang, Y. & Liu, C. T. Size-affected shear-band speed in bulk metallic glasses. *Appl. Phys. Lett.* **99**, 171904 (2011).
28. Georgarakis, K. *et al.* Shear band melting and serrated flow in metallic glasses. *Appl. Phys. Lett.* **93**, 031907 (2008).

Acknowledgement

This work was supported by World Premier International Research Center Initiative (WPI), MEXT, Japan.

Author contributions

Ketov S.V. and Louzguine-Luzgin D.V. wrote and corrected the manuscript text and figures. All authors reviewed the manuscript.

Additional information

Competing financial interests: The authors declare no competing financial interests.

How to cite this article: Ketov, S. V. & Louzguine-Luzgin, D.V. Localized shear deformation and softening of bulk metallic glass: stress or temperature driven? *Sci. Rep.* **3**, 2798; DOI:10.1038/srep02798 (2013).



This work is licensed under a Creative Commons Attribution-NonCommercial-ShareAlike 3.0 Unported license. To view a copy of this license, visit <http://creativecommons.org/licenses/by-nc-sa/3.0>